Research Article

Anna Maria Posadino#, Gian Luca Erre#, Annalisa Cossu, Costanza Emanueli, Ali H. Eid, Angelo Zinellu, Gianfranco Pintus*, Roberta Giordo*

NADPH-derived ROS generation drives fibrosis and endothelial-to-mesenchymal transition in systemic sclerosis: Potential cross talk with circulating miRNAs

https://doi.org/10.1515/bmc-2021-0023
received November 22, 2021; accepted January 17, 2022

Abstract: Systemic sclerosis (SSc) is an immune disorder characterized by diffuse fibrosis and vascular abnormalities of the affected organs. Although the etiopathology of this disease is largely unknown, endothelial damage and oxidative stress appear implicated in its initiation and maintenance. Here, we show for the first time that circulating factors present in SSc sera increased reactive oxygen species (ROS) production, collagen synthesis, and proliferation of human pulmonary microvascular endothelial cells (HPMECs). The observed phenomena were also associated with endothelial to mesenchymal transition (EndMT) as indicated by decreased von Willebrand factor (vWF) expression and increased alpha-smooth muscle actin, respectively, an endothelial and mesenchymal marker. SSc-induced fibroproliferative effects were prevented by HPMECs exposition to the NADPH oxidase inhibitor diphenyleneiodonium, demonstrating ROS's causative role and suggesting their cellular origin. Sera from SSc patients showed significant changes in the expression of a set of fibrosis/EndMT-associated microRNAs (miRNA), including miR-21, miR-92a, miR-24, miR-27b, miR-125b, miR-29c, and miR-181b, which resulted significantly upregulated as compared to healthy donors sera. However, miR29b resulted downregulated in SSc sera, whereas no significant differences were found in the expression of miR-29a in the two experimental groups of samples. Taking together our data indicate NADPH oxidase-induced EndMT as a potential mechanism of SSc-associated fibrosis, suggesting fibrosis-associated miRNAs as potentially responsible for initiating and sustaining the vascular alterations observed in this pathological condition.

Keywords: systemic sclerosis, fibrosis, oxidative stress, miRNAs, EndMT, NADPH

Introduction

Systemic sclerosis (scleroderma, SSc) is a complex multisystem autoimmune disease, of unknown etiology, characterized by an immune system dysregulation and progressive fibrosis of both skin and visceral organs, with prominent and severe vascular alterations [1]. Fibroproliferative vasculopathy affecting microvasculature leads to progressive damage, starting with vessel narrowing until the complete vascular obliteration [2]. Indeed, patients with SSc often exhibit early signs of vasculopathy in small blood vessels with nailfold capillaries changes (Raynaud's phenomenon) before the onset of clinical symptoms of tissue

# Equal contribution.

*** Corresponding author: Gianfranco Pintus,** Department of Biomedical Sciences, University of Sassari, 07100 Sassari, Italy; Department of Medical Laboratory Sciences, College of Health Sciences and Sharjah Institute for Medical Research, University of Sharjah, University City Rd, Sharjah 27272, United Arab Emirates, e-mail: gpintus@sharjah.ac.ae
*** Corresponding author: Roberta Giordo,** Department of Basic Sciences, College of Medicine, Mohammed Bin Rashid University of Medicine and Health Sciences, Dubai 505055, United Arab Emirates, e-mail: Roberta.Giordo@mbru.ac.ae
Anna Maria Posadino, Annalisa Cossu, Angelo Zinellu: Department of Biomedical Sciences, University of Sassari, 07100 Sassari, Italy
Gian Luca Erre: Rheumatology Unit, Department of Clinical and Experimental Medicine, University Hospital (AOUSS) and University of Sassari, 07100 Sassari, Italy
Costanza Emanueli: National Heart and Lung Institute, Imperial College London, Hammersmith Campus, London, W12 0NN England, United Kingdom
Ali H. Eid: Department of Basic Medical Sciences, College of Medicine, Qatar University Health, Qatar University, Doha, 2713, Qatar; Biomedical and Pharmaceutical Research Unit, Qatar University Health, Qatar University, Doha, 2713, Qatar

fibrosis [3]. Endothelial cells (ECs) activation and damage are recognized as the initial triggers of the SSc-associated fibrotic process. Indeed, endothelial dysfunctions and vascular anomalies consistently precede tissue fibrosis, suggesting a primary role of ECs in the pathogenesis and development of the disease [4,5]. In this contest, oxidative stress, besides being responsible for EC injuries and vascular complications [6], is emerging as a crucial player in SSc establishment and progression [7,8]. Reactive oxygen species (ROS) increase has been detected in different SSc patients' cells types, including fibroblast, monocytes, erythrocytes, and T lymphocytes [9–12]. In addition, ROS levels are higher in ECs and fibroblasts exposed to SSc sera than the healthy controls [13].

Fibrosis is the dominant aspect of SSc, and myofibroblasts, a population of mesenchymal cells, appear to be mainly responsible of the fibrotic processes in various organs [14]. Myofibroblasts' unique feature is the excessive deposition of connective molecules, including collagen and α-smooth muscle actin (α-SMA), which ultimately leads to abnormal tissue restructuring and organ dysfunction [15,16]. Besides deriving from fibroblasts, tissue-resident activated myofibroblasts can originate by trans-differentiation of other cell types such as pericyte, adipocyte, epithelial cells, and ECs [17].

In this regard, it is now becoming evident that ECs can differentiate into myofibroblasts through the endothelial to mesenchymal transition (EndMT) process, where they lose their typical endothelial phenotype and progressively acquire mesenchymal features. EndMT occurrence has been reported in the skin and lung of patients with SSc [18,19] as well as in a substantial number of animal models with SSc-associated pulmonary fibrosis and SSc-associated pulmonary arterial hypertension [20,21]. Oxidative stress and EndMT are, thus, important protagonists of vasculopathy and fibrosis, the two main pathological processes of SSc. A link between ROS and EndMT has been reported in several conditions, including SSc [22–27]. In this regard, oxidative stress mediates the conversion of ECs into myofibroblasts via transforming growth factor (TGF-β) secretion [28], which is also a potent EndMT inducer [29]. Nonetheless, the mechanisms underpinning this connection are still unclear.

By posttranscriptionally regulating gene expression, microRNAs (miRNAs), a class of evolutionarily conserved short non-coding RNAs (~22 nucleotides), play an essential role in SSc-associated vasculopathy and fibrosis [30,31]. miRNAs are also present into biological fluids where they act as mediators of cell-to-cell signaling [32,33]. In this regard, miRNAs have been reported involved in EndMT, and oxidative stress [22,23,34,35], and their expression is altered in SSc sera [36–38]. Nonetheless, a correlation between these phenomena in SSc remains to be elucidated.

We hypothesize that prooxidant circulating factors may trigger SSc-associated fibrotic processes, such as oxidative stress and EndMT and that miRNAs might be part of the complex molecular machinery driving this pathological phenomenon. To find answers to our research questions, we assessed oxidative status and EndMT occurrence in human pulmonary microvascular endothelial cells (HPMECs) upon exposure to SSc sera. Then we evaluated the sera of SSc patients and healthy donors (HD) for the expression levels of a set of SSc-associated miRNAs to investigate their potential connection with SSc-induced oxidative stress and Fibrosis/EndMT.

Materials and methods

Patient selection

Serum samples were collected from SSc patients at the Unit of Complex Rheumatology, Sassari. Table 1 summarizes the clinical and serological characteristics of the 16 patients enrolled in this study. All SSc patients met the SSc classification criteria of American College of Rheumatology (ACR)/European League Against Rheumatism (EULAR) [39]. The onset of the disease and the classification of patients having limited or diffuse were performed following the ACR/EULAR criteria for SSc classification [39]. All the previous medications were maintained during the study, whereas no other medications were started within the study framework. Posted flyers were used to recruit HD who were enrolled in the study after passing a screening questionnaire to exclude any underlying vascular or autoimmune condition.

Ethical approval: The research related to human use has been complied with all the relevant national regulations, institutional policies, and in accordance the tenets of the Helsinki Declaration and has been approved by the Ethics Committee of the Azienda Sanitaria Locale #1 of Sassari with protocol # 779/L 2009.

Informed consent: Informed consent has been obtained from all individuals included in this study.

Cell culture

The HPMECs used in this study were obtained from human lungs of HD and were supplied by Innoprot (Innoprot, Bizkaia, Spain). HPMECs were cultured in a specific basal medium supplemented with EC growth

Table 1: Clinical characterization of the enrolled SSc patients

Variables	SSc (n = 16)	HD (n = 14)
Age at serum sampling (years)*	55 ± 11	54.1 ± 10.4
Sex		
Women	12 (75)	12 (86)
Men	4 (25)	2 (14)
Race		
White	15 (94)	11 (79)
Black	0	3 (21)
Smoking status		
Never	7 (44)	10 (71)
Current	5 (31)	4 (29)
Past	4 (25)	
SSc types		
Diffuse	11 (69)	
Limited	5 (31)	
SSc duration (years)*	13 ± 12.3	
Autoantibody status		
Anti-RNA polymerase 3	2 (13)	
Anti-Scl-70	10 (63)	
Anti-ACA	2 (13)	
Medication use (current)		
Immunosuppressants ‡	2 (13)	
Calcium channel blocker	8 (50)	
Endothelin receptor antagonist	2 (13)	
Phosphodiesterase 5 inhibitor	2 (13)	
Prostanoid	10 (63)	
Statin	1 (6)	
Aspirin	4 (25)	

All values are given as numbers (%) unless otherwise specified. *Mean ± SD. SSc, systemic sclerosis; HD, healthy donors; ACA, anticentromere antibody; Scl-70, topoisomerase I; ‡ use of immunosuppressants include cyclophosphamide, mycophenolate, methotrexate, hydroxycholorquine, or prednisone.

supplements as per the supplier's directions. At confluency, HPMECs were subcultured at a split ratio of 1:2 and used within three/four passages. Unless specified in the text, in all experiments, cells have been grown in 96-well black plates (BD Falcon, Franklin Lakes, New Jersey, United States) and treated with basal medium containing 10% (v/v) of the subjects' sera. Sera among the different subjects were normalized based on protein content [40,41]. In selected experiments, HPMECs were pretreated with broad NADPH inhibitor diphenyleneiodonium (DPI) chloride to investigate the involvement of NADPH oxidase in the observed phenomena [42].

Measurement of intracellular ROS

The ROS fluorescent molecular probe 2′,7′-dichlorodihydrofluorescein diacetate (H_2-DCFDA) was used to assess the intracellular ROS levels [43,44]. Inside the cell, after removal of the acetate groups by intracellular esterases, the nonfluorescent molecule is converted to a green-fluorescent form on oxidation in the presence of ROS. HPMECs were incubated for 30 min with phosphate-buffered saline (PBS) containing 1 μM H_2-DCFDA, washed with PBS, and treated as described. Fluorescence intensity was measured by using a Tecan GENios Plus microplate reader (Tecan, Switzerland) in a light-protected condition, at the excitation wavelength of 485 nm and an emission wavelength of 535 nm. The treatment-induced variation of fluorescence was kinetically measured over a time course of 5 h. All fluorescence measurements were corrected for the background fluorescence and protein concentration. Results were evaluated by comparing five measurements and expressed as a means ± standard deviation (SD) of the relative fluorescence unit (RFU) values.

Determination of cell proliferation

Cell proliferation was assessed by using the BrdU assay (Roche CH), a chemiluminescent immunoassay based on the determination of BrdU incorporation during DNA synthesis [45,46]. When cells are exposed to BrdU, the compound is incorporated into the newly synthesized DNA strands of actively proliferating cells. DNA-incorporated BrdU can be measured using anti-BrdU antibodies, allowing the assessment of the DNA synthesizing cells. Subconfluent HPMECs were treated for 48 h with 10% (v/v) of serum from different subjects. BrdU was added 12 h before the end of the experiments, then the supernatant was removed, and cells were fixed for 30 min with a fixing-denaturating solution (Fix-Denat). At the end of incubation time, the Fix-Denat solution was discarded, and the cells were incubated for 90 min with a horseradish peroxidase-conjugated anti-BrdU antibody. After three washing, the substrate solution was added and allowed to react for 3–10 min at room temperature. Within this time window, the horseradish peroxidase catalyzes the oxidation of diacylhydrazide, and the reaction product, decaying from its excited state, yields light. Finally, a GENios Plus microplate reader (Tecan) was used to read the light emission of treated cells. Results were expressed as a means ± SD of the relative light units/s (RLU/s) values.

Production of lentiviral particles

To assess the human collagen type-I (COL1A1) synthesis, a set of lentiviral particles was created and used to transduce HPMECs exposed to the different experimental

treatments [24]. Specifically, the following lentivectors were used to produce the infecting lentiviral particles: pCOL1A1-turbo Green Fluorescent Protein (tGFP), a plasmid containing the green fluorescent protein (GFP) driven by the human COL1A1 promoter; pEFα-LV-FP602, a plasmid containing the red fluorescent protein (FP602) driven by the elongation factor 1-alpha (EFα), which is a constitutive promoter. pCOL1A1-tGFP activation is associated with collagen synthesis, whereas the activation of pEFα-LV-FP602 expresses the red protein FP602 used as a control for normalizing the cell transduction efficiency. Transient transfection of the 293T/17 packaging cells was used to produce the lentiviral particles [25,47]. Briefly, 70% confluence 293T/17 cells were mixed with the transgene expression plasmid (pCOL1A1-tGFP or EFα-FP602), and then the second generation packaging plasmids (pMD2.G and pCMVR8.74) were used to transfect the cells. A calcium-phosphate solution consisting of a 1:1 mixture of 0.25 M of CaCl2:2X BBS (0.28 M NaCl, 0.05 M *N*,*N*-bis-(2-hydroxyethyl)-2-aminoethanesulfonic acid, 1.5 mM Na_2HPO_4) was used to transfect the cells. The medium was changed 12–16 h posttransfection, and virus-containing media was harvested twice at 24 and 48 h after changing the medium. The particle-containing medium was centrifuged for 2 h at 19,400 rpm in a L8-80M ultracentrifuge (Beckman, Brea, California, United States), and then, the pellet was washed in 1 mL Hanks' Balanced Salt Solution (HBSS) and centrifuged again for 2 h at 21,000 rpm in a L8-80M ultracentrifuge (Beckman). The final pellet was resuspended in 200 µL of HBSS, vortexed for 2 h before being stored at −80°C in 20 µL aliquots. Virus titer was assessed by using the p24 ELISA kit (PerkinElmer, Waltham, Massachusetts, United States) according to the manufacturer instruction.

Generation of HPMEC/pCol1GFP-pEFα-FP602 cell lines

Experiments were performed on stable transfected HPMECs containing pCOL1A1-tGFP and EFα-FP602 [48,49]. In brief, the produced lentiviral particles were used to transduce 50–60% confluent HPMECs using an optimized multiplicity of infection to reach an infection efficiency of about 95%. To this end, cells were incubated for 24 h with the lentiviral particles; then, an equal amount of free-virus fresh medium was added for another 24 h. At the end of the transfection process, a flow cytometer analysis was performed to assess the infection efficiency. The obtained stable transduced HPMECs were then used for determining the variations of COL1A1 synthesis under the different experimental conditions.

Collagen determination

COL1A1 synthesis was assessed using the created HPMEC/pCol1GFP-pEFα-FP602 stable cell lines. We used this specific method as it allowed us to per a real-time determination of multiple samples in a 96-well plate using small aliquots of subject sera [24,40,41]. The stable transfected HPMEC/pCol1GFP-pEFα-FP602 cell line was stimulated with basal medium containing 10% sera from HD and 10% (v/v) of sera from SSc patients (SSc). Potential variation of GFP fluorescence induced by the treatments was kinetically assessed over a time-course of 4 h using a Tecan GENios Plus multiplate reader (Tecan, Mannedorf, Switzerland). Fluorescence quantification was performed using 485 and 535 nm as excitation wavelengths and 535 and 590 nm as emission wavelengths, respectively, for pCOL1A1-LV-tGFP and EFα-LV-FP602, and pCOL1A1-LV-tGFP to EFα-LV-FP602 ratio was used to normalize the data for the transduction efficiency. Data were then expressed as a means ± SD of the RFU values.

Protein extraction

HPMECs were grown in T12.5 culture flasks (BD Falcon). Subconfluent cells were treated with 10% (v/v) sera from HD subjects and SSc patients for 72 h. After the treatment, cells were washed with chilled PBS and then incubated in ice-cold lysis buffer (CytoBuster; Novagen, Darmstadt, Germany) containing protease and phosphatase inhibitors (Sigma, St Louis, MO) for 10 min at 4°C. Cells were then scraped, and the lysate was centrifuged at 16,000*g* for 5 min at 4°C. The supernatant was collected and stored in the same lysis buffer at −80°C. Protein content was measured using the Bradford assay as per the manufacturer's protocol (Sigma, St Louis, MO).

Determination of alpha-smooth muscle actin (α-SMA) and von Willebrand factor (vWF)

Variation of α-SMA and vWF protein expression in response to sera treatment was quantitatively assessed as previously described by enzyme immunoassay [41]. Briefly, after 48 h of treatment with the sera, HPMECs were washed and collected in the proteins extraction buffer. A total of 100 µL of peroxidase-labeled anti-α-SMA and peroxidase-labeled anti-vWF monoclonal antibody solutions were transferred, respectively, into anti-α-SMA and vWF monoclonal

antibody-coated wells. Subsequently, 20 µL of cell extract or standard was added, then the solution was incubated for 3 h at 37°C. Then 100 µL of substrate solution was added to each well. The reaction between the peroxidase-labeled anti-α-SMA and -vWF monoclonal antibodies and substrate results in color development that yield an intensity proportional to the quantity of α-SMA and -vWF present in samples and standards. Finally, 100 µL of stop solution was added to each well after 15 min of incubation at room temperature. The amount of α-SMA and vWF was quantitated by measuring the absorbance (450 nm) using a Tecan GENios Plus microplate reader (Tecan, Switzerland). Then, the concentrations of the two target proteins in the samples were determined by comparing their specific absorbances with those obtained for the standards plotted on a standard curve. All samples were normalized for protein content before proceeding with the ELISA determination. Results were expressed as a means ± SD of ng/mL protein.

RNA isolation and quantitative real-time polymerase chain reaction (PCR)

Total RNA was extracted using the miRNeasy kit (Qiagen, Hilden, Germany), according to the manufacturer's instructions, with minor adjustments. For RNA extraction, 200 µL of the sample (serum) was used with 1 mL of QIAzol. 10 µL (from a 5 fmol/mL stock) of a synthetic analog of the non-human *Caenorhabditis elegans* microRNA-39 (celmiRNA-39; Qiagen) was spiked to normalize RNA extraction efficiency. The TaqMan miRNA reverse transcription kit and the miRNA-specific stem-loop primers system (Thermo Fisher Scientific) were used to perform individual miRNAs reverse transcription. The qPCR was performed in triplicate using 2× Universal PCR Master Mix with No AmpErase UNG (Thermo Fisher Scientific) using the QuantStudio 6 Flex Real-Time PCR System (Thermo Fisher Scientific). Cel-miRNA-39 was used to normalize the expression of the studied miRNA [45,50].

Bioinformatic analysis

miRecords was used to determine the potential target genes of selected miRNAs. This database consists of two components: validated targets and predicted targets. The first is a database of experimentally validated miRNA targets resulting from literature. In contrast, the predicted targets is a database of predicted miRNA targets produced by integrating 11 established miRNA target prediction programs [51]. To localize miRNAs targets in signaling pathways, we used miTALOS database [52]. Finally, we used miRwayDB [52] to evaluate miRNAs–pathways association, a database providing comprehensive information of experimentally validated target genes and microRNA–pathway associations in various pathophysiological conditions.

Statistical analysis

Kruskall–Wallis one-way analysis of variance, followed by a *post hoc* Dunn's test for multiple comparisons, was used to detect differences among the studied groups. When appropriate, a two-way analysis of variance, followed by a *post hoc* Šídák's test for multiple comparisons, was used to detect differences among studied groups. Differences between two groups were detected using the Mann–Whitney–Wilcoxon test. All statistical analyses were performed using GraphPad Prism version 9.00 for Windows (GraphPad Software, San Diego, CA, USA), and p-values <0.05 were considered statistically significant.

Results and discussion

SSc sera elicit an NADPH oxidase-dependent increase of ROS production in HPMECs

A growing number of evidence underline the role of oxidative stress in SSc pathogenesis [8,53]. Besides contributing to the disease prolongation, high ROS levels are also the leading cause of endothelial dysfunction [6], which appears to trigger many events underpinning SSc-associated vasculopathy [54]. We earlier reported that the exposition of human pulmonary vascular smooth muscle cells to sera of SSc patients elicited an NADPH oxidase-mediated ROS increase responsible for collagen synthesis overexpression [40]. Here, we hypothesize that a similar mechanism implicating ECs may be involved in SSc-associated vascular damage and fibrosis. As pulmonary fibrosis is the primary cause of mortality in SSc [55], HPMECs have been used in this study. For intracellular ROS levels detection, subconfluent HPMECs were loaded with 10 µM H_2-DCFDA and then cultured in basal medium containing 10% (v/v) of sera from both SSc patients and healthy donor (HD). Variations in intracellular ROS levels were kinetically

determined in an 8 h time-course experiment (Figure 1a), and values at 2 h were used for comparison (Figure 1b). Fluorescence data were normalized for protein content and expressed as RFU. As reported in Figure 1a, intracellular ROS levels in SSc-treated HPMECs were significantly higher than those observed in cells exposed to HD sera, suggesting that SSc patients harbor circulating factors able of increasing ECs' intracellular oxidative status. Moreover, the SSc sera-induced ROS increase appears to be mediated by NADPH oxidases, as cell pretreatment with the broad NADPH inhibitor DPI significantly attenuated the observed surge of ROS (Figure 2b).

NADPH oxidase-derived ROS mediate increased proliferation in HPMECs exposed to SSc sera

In physiological conditions, the endothelium is genetically stable and remains in a quiescent state for a prolonged time [56]. Nonetheless, ECs own the ability to promptly switch to a migratory or proliferative status when activated by proangiogenic or proinflammatory stimuli [57]. In SSc, the overproduction of ROS is responsible for endothelial dysfunction and for promoting a profibrotic and proinflammatory state [8,22,54]. Indeed, based on their concentration, ROS can be important modulators of physiological and pathological cell proliferation. For instance, while persistent ROS production can generally induce apoptosis through JNK pathway activation, a transient increase of ROS levels can elicit cell proliferation through extracellular signal-regulated kinase (ERK) pathway activation [58]. In the attempt to understand whether the observed variations of intracellular ROS could affect HPMECs proliferation, we assessed the rate of DNA synthesis in cells exposed to SSc and HD sera for both 24 and 48 h. As depicted in Figure 2a, a significant increase in cell proliferation was elicited by SSc sera compared to HD sera. Moreover, similarly to data in Figure 1b, NADPH inhibition significantly blunted the increase in cell proliferation elicited by SSc sera (Figure 2b). Besides being consistent with the SSc fibro-proliferative features, this finding confirms the relationship between ROS and cell proliferation, suggesting NADPH-activating prooxidant factors underpinning SSc-induced ROS and proliferation increment observed in HPMECs treatment with SSc sera.

NADPH oxidase-derived ROS mediates increased collagen synthesis in HPMECs exposed to SSc sera

Among the connective macromolecules, a persistent collagen overproduction is primarily responsible for the progressive nature of SSc fibrosis [59]. Although activated myofibroblasts appear to be the primary source of collagen in SSc, it is becoming evident that also ECs play an important role in the disease-associated tissue restructuring by synthesizing collagen and contributing to vessel/

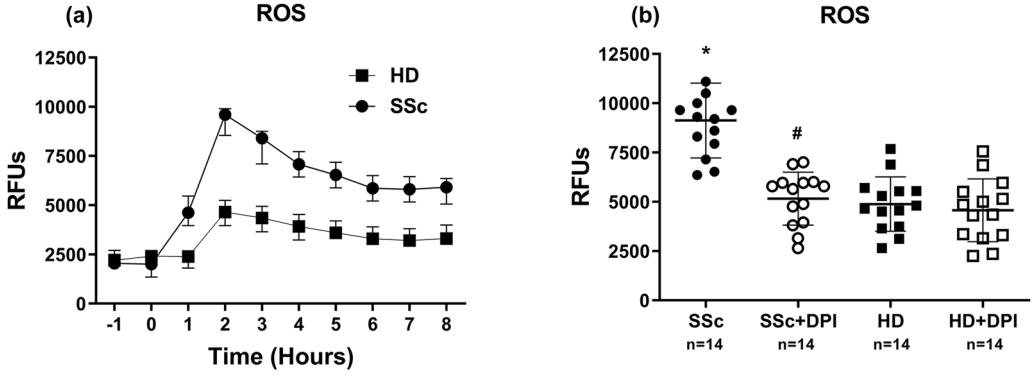

Figure 1: Effect of SSc sera on HPMEC intracellular ROS levels: (a) SSc sera increase intracellular ROS production in HPMEC. The real-time assessment of intracellular ROS production in HPMECs exposed to sera of SSc patients and healthy donor. Before sera stimulation, subconfluent HPMECs were loaded with 10 μM of H_2-DCFDA and then cultured in basal medium containing 10% (v/v) of sera from SSc patients (SSc) and healthy donor (HD). Variations in intracellular ROS levels were kinetically determined in an 8 h time-course (a randomly selected representative experiment is reported) and values at 2 h were used for comparisons in B. (b) SSc sera-induced ROS increase in HPMECs is mediated by NADPH oxidases. Before sera stimulation, subconfluent HPMECs were loaded with 10 μM of H_2-DCFDA and then cultured for 8 h in basal medium containing 10% (v/v) of sera from SSc patients and HD, then values at 2 h were used for comparisons. In selected experiments, H_2-DCFDA-loaded subconfluent HPMECs were preincubated for 1 h with 5 μM of NADPH oxidase inhibitor DPI before sera stimulation. Fluorescence data were normalized for protein content and expressed as mean ± SD of the RFUs. (b) Horizontal lines indicate the mean value and standard deviation range. Kruskall–Wallis one-way analysis of variance, followed by a *post hoc* Dunn's test for multiple comparisons, was used to detect differences among studied groups. *$p \leq 0.001$, significantly different from the control group (HD); #$p \leq 0.0001$, significantly different from the SSc group.

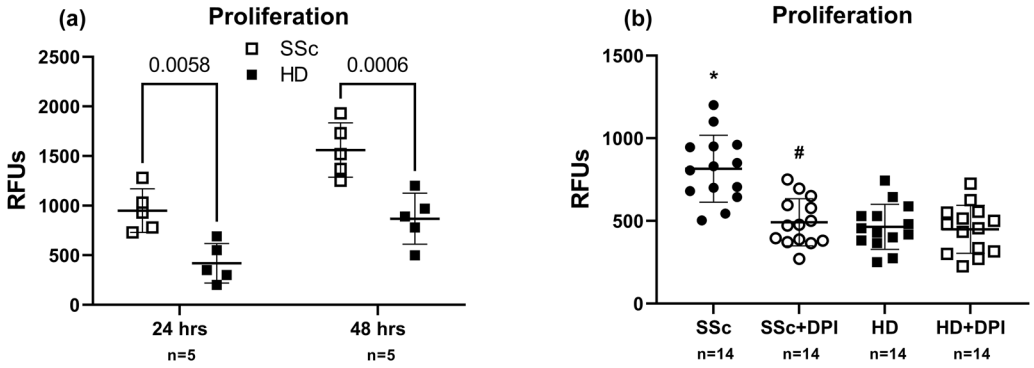

Figure 2: Effect of SS sera on HPMECs proliferation: (a) SSc sera induce HPMECs proliferation. Subconfluent HPMECs were cultured for 24 and 48 h in basal medium containing 10% (v/v) of sera from SSc patients and healthy donor. (b) SSc sera-induced proliferation increase in HPMECs is mediated by NADPH oxidases. Subconfluent HPMECs were cultured for 48 h in basal medium containing 10% (v/v) of sera from SSc patients and healthy donor. In selected experiments, cells were incubated for 1 h with 5 μM of the NADPH oxidase inhibitor DPI before exposure to the sera. Fluorescence data were normalized for protein content and expressed as mean ± SD of the RFUs. (a) Horizontal lines indicate the mean value and standard deviation range. Two-way analysis of variance, followed by a *post hoc* Šídák's test for multiple comparisons, was used to detect differences among studied groups. (b) Horizontal lines indicate the mean value and standard deviation range. Kruskall–Wallis one-way analysis of variance, followed by a *post hoc* Dunn's test for multiple comparisons, was used to detect differences among studied groups. *$p \leq 0.0004$, significantly different from the control group (HD); #$p \leq 0.002$, significantly different from the SSc group.

microvessel narrowing [60]. In this light, we investigate whether circulating prooxidant factors present in SSc sera could contribute to the SSc-associated fibrotic phenotype by augmenting the synthesis of collagen type 1 (COL1A1). COL1A1 synthesis, in both the presence of SSc and HD sera, was detected using the HPMEC/pCol1GFP-pEFα-FP602 cell line, obtained by the cotransduction of HPMECs with both pCOL1A1-tGFP and pEFα-FP602 lentiviral particles [24,40]. This technique offers the advantage of kinetically assessing multiple samples simultaneously in a 96-well plate using small amounts of subject sera. As indicated in Figure 3a, the exposure of HPMECs to SSc sera resulted in a progressive

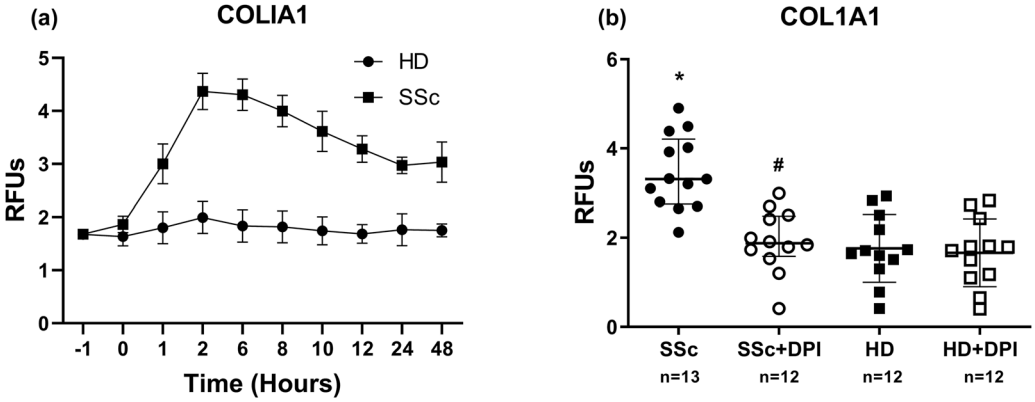

Figure 3: Effects of SSc sera on HPMECs collagen (COL1A1) promoter activation. (a) SSc sera induce HPMECs collagen synthesis. Subconfluent HPMECs were transduced with lentiviral particles obtained from the COL1A1-LV-tGFP and EF1α-LV-FP602 lentivectors, and then cultured in basal medium containing 10% (v/v) of sera from SSc patients (SSc) and healthy donor (HD). Variations of COL1A1 promoter activation were kinetically followed for 48 h (a randomly selected representative experiment is reported) and values at 8 h were used for comparison in B. (b) SSc sera-induced COLIA1 increase in HPMECs is mediated by NADPH oxidases. Before sera stimulation, subconfluent HPMECs were transduced with lentiviral particles obtained from the COL1A1-LV-tGFP and EF1α-LV-FP602 lentivectors and then cultured for 48 h in basal medium containing 10% (v/v) of sera from SSc patients and HD; then values at 2 h were used for comparisons. In selected experiments, viral-transduced HPMECs were preincubated for 1 h with 5 μM of the NADPH oxidase inhibitor DPI before sera stimulation. (a) and b) Data are expressed as normalized transduction efficiency by reporting the mean ± SD of the RFUs ratio of COL1A1-LV-tGFP to EF1α-LV-FP602. (b) Horizontal lines indicate the mean value and standard deviation range. Kruskall–Wallis one-way analysis of variance, followed by a *post hoc* Dunn's test for multiple comparisons, was used to detect differences among studied groups. *$p \leq 0.0005$, significantly different from the control group (HD); #$p \leq 0.005$, significantly different from the SSc group (SSc).

time-dependent increase of the COL1A1 promoter activity with values at 2 h significantly higher in cells exposed to SSc sera compared to HD sera (Figure 3a and b). As found for the proliferation (Figure 2a), also the SSc-induced increase of COL1A1 synthesis appeared to be mediated by NADPH-activating prooxidant factors as it was significantly counteracted by DPI (Figure 3b).

NADPH oxidase-derived ROS mediates EndMT in HPMECs exposed to SSc sera

Besides being involved in extracellular matrix (ECM) remodeling, collagen is tightly linked to EMT and EndMT [61,62]. Moreover, as earlier mentioned, activated myofibroblasts appear to be the primary cells involved in SSc-associated fibrosis [21,63], and ECs represent a very likely source of myofibroblasts originated through EndMT. Emerging evidence also indicate a link between oxidative stress and EndM in SSc; in fact, antioxidants reduce EndMT in this disease while oxidative stress mediates its onset and progression [22]. These evidences, along with the increase of ROS and cell proliferation observed following exposure to SSc sera, led us to hypothesize that HPMECs may undergo an EndMT-like mesenchymal transformation, elicited by sera-contained prooxidant factors. During EndMT, ECs progressively lose their typical endothelial markers, acquiring a mesenchymal phenotype [64]. To gain molecular insights on our hypothesis, we checked the protein levels of α-SMA and vWF in HPMECs exposed to both SSc and HD sera. Indeed, α-SMA and vWF are two typical mesenchymal and endothelial markers, respectively. Although α-SMA is essential for the cell contractile activity [14,65], vWF plays a key role in the endothelium pathophysiology by recruiting platelets into the sites of vascular injury [66]. Protein levels of both α-SMA and vWF were assessed by ELISA in HPMECs exposed for 2 days to sera from SSc patients and HD. Consistently with the establishment of EndMT, significant alterations of the two proteins expression were detected. Indeed, α-SMA levels were higher in cells exposed to SSc sera than cells exposed to HD (Figure 4a), whereas a lower expression vWF was noted in cells exposed to SSc sera compared to cells exposed to HD (Figure 4b). Similarly to COL1A1 (Figure 3b), the pretreatment of HPMECs with DPI significantly blunted SSc sera-induced EndMT, indicating the involvement of NADPH-activating prooxidant factors in the observed process.

SSc sera contain profibrotic and EndMT associated miRNAs

Recent studies reported an association between miRNAs and ROS in vascular diseases [67], indicating miRNAs' ability to modulate redox-regulated pathways involved in

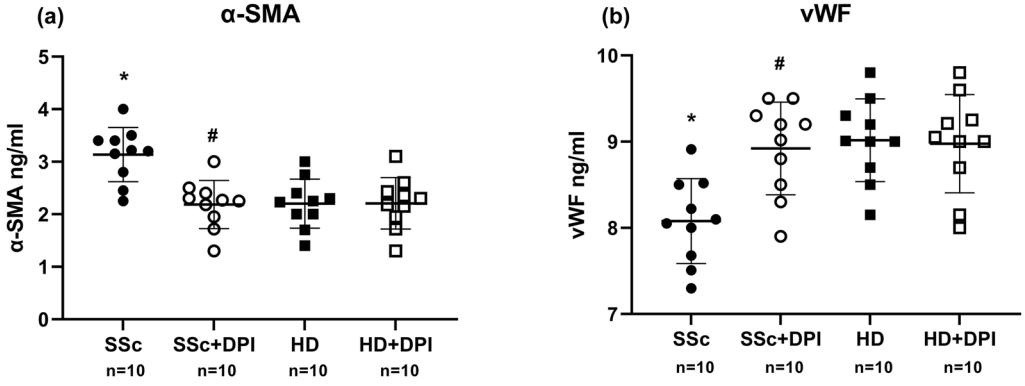

Figure 4: Effects of SSc sera on EndMT markers expression in HPMECs (a) SSc sera induce α-SMA expression in HPMECs. (b) SSc sera inhibits vWF expression in HPMECs. (a and b) Subconfluent HPMECs were cultured for 48 h in basal medium containing 10% (v/v) of sera from SSc patients (SSc) and healthy donor (HD). Cells were then processed for the determination of both α-SMA and vWF as reported in the material methods. In selected experiments, HPMECs were preincubated for 1 h with 5 μM of the NADPH oxidase inhibitor DPI before sera stimulation. (a and b) Data are expressed as nanogram per milliliter of protein. Horizontal lines indicate the mean value and standard deviation range. Kruskall–Wallis one-way analysis of variance, followed by a *post hoc* Dunn's test for multiple comparisons, was used to detect differences among studied groups. (a) *$p \leq 0.006$, significantly different from the control group (HD); #$p \leq 0.008$, significantly different from the SSc group (SSc). (b) *$p \leq 0.01$, significantly different from the control group (HD); #$p \leq 0.02$, significantly different from the SSc group (SSc).

cardiac and pulmonary diseases [68,69]. Indeed, miRNAs have been reported to be essential regulators of NADPH oxidase-mediated angiogenic response and modulators of the expression of genes involved in EndoMT [23,70–72]. These evidences suggest miRNAs may represent a mechanistic connection between ROS, endothelial dysfunctions, and SSc-associated fibroproliferative alterations. Therefore, we speculated that SSc patients' sera contain profibrotic miRNAs, which may drive the currently observed *in vitro* phenomena and thus be involved in SSc-associated vascular damage and fibrosis *in vivo*. To test our hypothesis, we investigated the serum content of nine miRNA (miR-21; miR-24; miR-181b; miR-92a; miR-27b; miR-29 a,b,c; and miR-125b) implicated in SSc pathogenesis and altered in sera/tissues of SSc patients [38,73,74]. The relative levels of all detected miRNAs are shown in Figure 5. We found most of the miRNAs significantly increased in the SSc patients' sera compared to normal sera, except for miR-29b and miR-29a, which were instead, decreased (miR-29b), and not significantly altered (miR-29a; Figure 5). Combining information obtained by both in silico analysis (by miRNA targets/pathway prediction tools) and literature data, these altered miRNAs appeared linked to a signaling cross-talk between ROS and a set of pathways involved in the pathophysiological processes of fibrosis such as TGF-β/SMAD, PI3K/AKT, and ERK/MAP. Moreover, most of these miRNAs have also been validated for being involved in the overdeposition of ECM components, EndMT, and oxidative stress. Table 2 summarizes the known information related to the miRNAs detected in this study. For instance, miR-21 has been reported linked to all the above-mentioned fibrotic pathways [75], and it might thus play a significant role in driving the phenomena we observed following HPMEC treatment with SSc sera. Indeed, the overexpression of miR-21

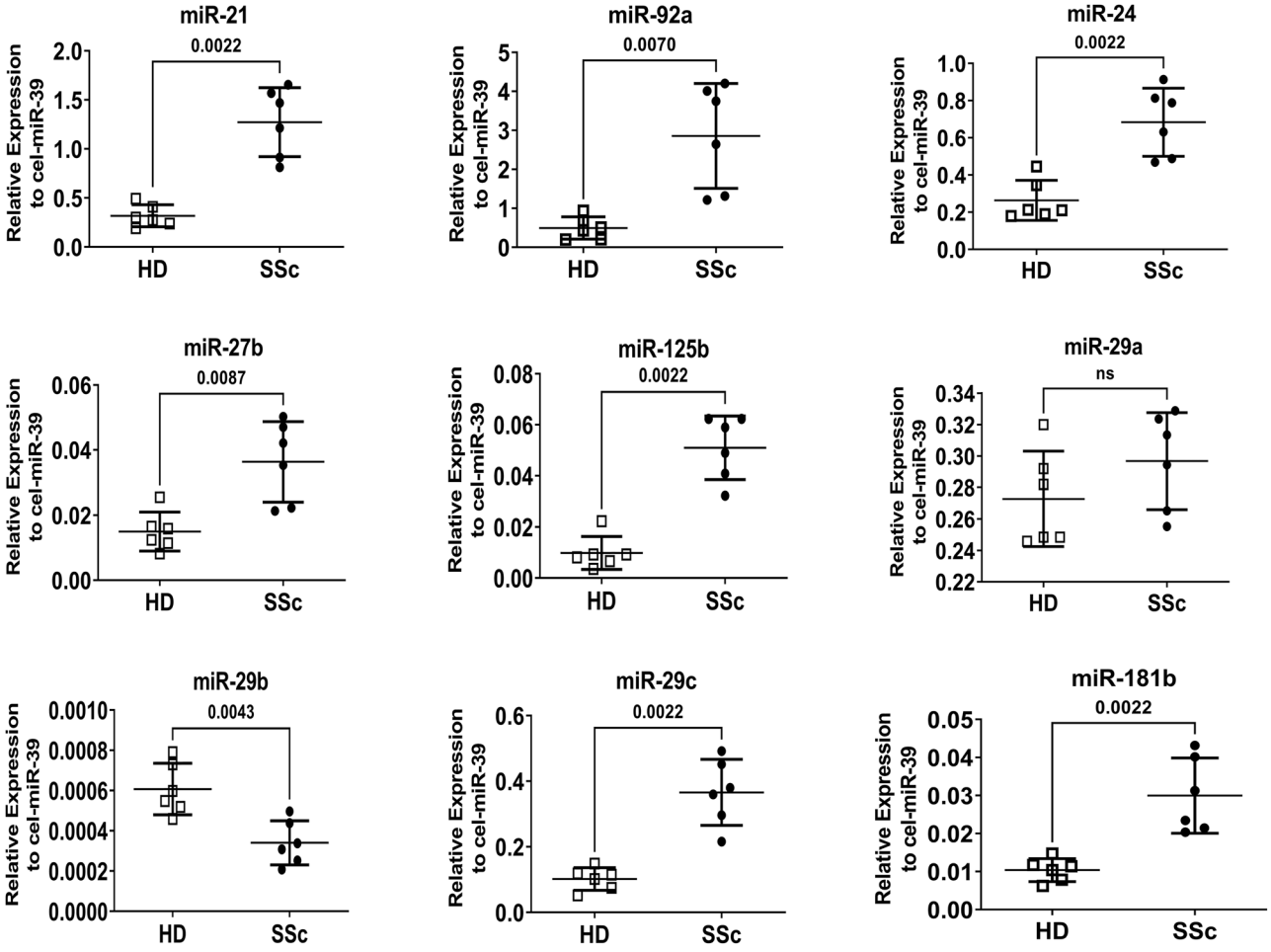

Figure 5: Content levels of miRNAs present in serum of HD and SSc patients. The expression of the indicated microRNAs (miRNAs) was measured (real-time quantitative polymerase chain reaction) in the serum of healthy donor (HD) and SSc patients (SSc) samples. miRNA levels as expressed as relative expression normalized to levels of cel-miRNA-39. Horizontal lines indicate the mean value and standard deviation range. Mann–Whitney test was used to detect differences among HD and SSc groups.

Table 2: Summary of the known information related to the miRNAs detected in this study

	miR-21	miR-181b	miR-29a	miR-29b	miR-29c	miR-24	miR-92a	miR-27b	miR-125b
Validated targets (miRecords)	TGFBR2 TIMP3	TIMP3 GATA6	COL2A1 COL3A1 PTEN	COL1A1 COL2A1 COL3A1 MMP2 TCL1A	COL1A1 COL1A2 COL3A1 COL4A1 COL4A2 COL15A1	MAPK14 ACVR1BA			
Predicted targets (miRecords)	SMAD7 SPRY1 TGFBI	TGFBI	SPRY1	SPRY1	PTEN		COL12A1 SMAD7		
Experimentally validated targets	PTEN			AKT3			PTEN MMP-I	ET-1	
Signaling pathways	TGF-β/Smad PI3K-Akt MAPK	TGFβ/Smad	PI3K-Akt MAPK	PI3K-Akt MAPK	MAPK	MAPK	PI3K-Akt		
Biological processes	Fibrosis EndMT ROS		Fibrosis EndMT ROS	Fibrosis EndMT ROS	Fibrosis EndMT ROS	Fibrosis EndMT ROS	Fibrosis EndMT	EndMT ROS	Fibrosis ROS

decreases Smad7, a negative TGF-β regulator, thus activating TGF-β-induced ECM production and consequently increasing fibrosis [76]. However, TGF-β1 and Smad3 upregulate miR-21 expression, which in turn activates TGF-β/Smads signals [77–80]. Additionally, via modulation of the tissue inhibitor of metalloproteinases 3 (TIMP3) activity, TGF-β1 regulates fibrosis by promoting ECM production and inhibiting ECM degradation [81]. Similarly to TGF-β1, miR-21 might regulate the fibrotic process by the same dual mechanism. Indeed, in SSc, miR-21 regulates the expression of genes responsible for ECM production, such as collagen, fibronectin, and α-SMA, and *TIMP-3* is one of the most validated miR-21 target genes [76]. *TIMP-3* is also a target gene of miR-181b, which we found increased in SSc sera along with miR-21. Besides the TGF-β/Smads pathway, PI3K/AKT and ERK/MAPK are also two miR-21-regulated signaling pathways involved in fibrosis pathophysiology [75]. In the ERK/MAPK-mediated fibrosis, both miR-21 and miR-29a-b target the sprouty (Spry) genes, which encode potent ERK/MAPK inhibitors. However, they play opposite roles as miR-21 is a Spry inhibitor and hence activates ERK/MAPK-associated fibrosis, whereas miR-29a-b are activators and, therefore, block the fibrotic process mediated by ERK/MAPK [82]. This aspect is consistent with our results reporting the increased expression of miR-21 and downregulation of miR-29a-b in SSc sera. Our current results showing increasing cell proliferation, collagen synthesis, and α-SMA expression on HPMECs treatment with SSc sera (Figures 2–4) appear to be EndMT-associated events ascribable to the ECs differentiation into myofibroblasts. PI3K/AKT signals are also involved in EMT and EndMT [83,84], and miR-21 might regulate EndMT through this signaling pathway. Indeed, the endogenous inhibitor of AKT activation, phosphatase, and tensin homolog (PTEN) is inhibited by miR-21 [85,86]. Moreover, PTEN is also a target of miR-92a (overexpressed in SSc sera), which has been reported to increase cell proliferation and promote EndMT and EMT [87–89]. miR-92a can also regulate collagen accumulation by downregulating the metalloproteinase-1, a protein involved in ECM breakdown [74,90].

miR-29a, miR-29b, and miR-29c also play an important role in collagen synthesis regulation. In fact, this miRNAs family, besides being altered in SSc sera/plasma and involved in the fibrotic process [73,91], also targets most collagen encoding genes. In this regard, our current findings show miR-29c upregulated, whereas miR-29b and miR-29a are respectively downregulated and not significantly altered. The interplay between the members of this miRNA family is still unclear, but it has been suggested that miR-29a and miR-29b are collagen synthesis repressors, whereas miR-29c is an activator [92]. We believe that a similar mechanism might be responsible for the increased collagen synthesis observed upon HPMECs exposition to SSc sera.

By activating the TGF-β pathway, miR-24 and miR-27b, two other miRNAs that we found upregulated in SSc sera, are positive regulators of EndMT [93]. In addition, miR-27b is either target or regulator of endothelin-1 (ET-1), a potent vasoconstrictor secreted by ECs and involved in SSc pathophysiology [94–96]. A similar regulatory mechanism has been reported between ROS and ET-1, where ROS can

increase ET-1 production [97,98] and ET-1 can, in turn, increase ROS levels [54,99]. In SSc, ROS modulate most of the key components involved in the disease pathophysiology, including pathways related to the fibrotic process [8]. For instance, TGF-β and ROS show a reciprocal regulation in fibrosis induction [100], ROS can induce EMT via the TGF-β1/PI3K/Akt/pathway [101], and the ERK/MAPK pathway can be activated by increased ROS [102]. Interestingly, most of the miRNAs we analyzed in SSc sera are implicated in the same pathways, and some of them (miR-21, miR-24, miR-125b, and miR-29b) can increase ROS levels or being modulated by ROS [103–106]. Considering our experimental results, the in-silico analysis, and the literature, data suggest that miRNAs present in the patients' sera could drive EndMT in SSc by interacting with the intracellular redox system and regulating fibrosis through a cross talk among the three main fibrosis-associated signaling pathways.

Conclusion

Our data suggest EndMT as a potential mechanism of SSc-associated fibrosis, indicating NADPH oxidase-induced oxidative stress as its triggering event. This study also supports the hypothesis that prooxidant circulating factors, including miRNAs, could be responsible for initiating and sustaining endothelial dysfunction in SSc driving disease-associated vascular alterations.

Acknowledgements: This study has been made possible thanks to grants from the University of Sharjah (Seed 2001050151, collaborative 2101050160), fondo UNISS di Ateneo per la Ricerca 2020, and Fondo di Sviluppo e Coesione 2014–2020, Patto per lo Sviluppo della Regione Sardegna, L.R.7-2017-RASSR82005.

Funding information: University of Sharjah (Seed 2001050151, collaborative 2101050160), fondo UNISS di Ateneo per la Ricerca 2020, and Fondo di Sviluppo e Coesione 2014–2020, Patto per lo Sviluppo della Regione Sardegna, L.R.7-2017-RASSR82005.

Author contributions: Conceptualization, R.G., G.L.E., C.E., and G.P.; methodology, R.G., A.M.P., A.C., A.Z., C.E., and G.P.; project administration, G.L.E., A.Z., and G.P.; resources, G.L.E., A.M.P., A.C., A.Z. A.H.E., C.E., and G.P.; writing – original draft, R.G., A.M.P., and G.P.; and writing – review and editing, R.G., A.Z., G.L.E., A.H.E., and G.P. All authors have read and agreed to the published version of the manuscript.

Conflict of interest: Authors state no conflict of interest.

Data availability statement: The datasets generated during and/or analyzed during the current study are available from the corresponding author on reasonable request.

References

[1] Denton CP, Khanna D. Systemic sclerosis. Lancet. 2017;390:1685–99.
[2] Varga J, Abraham D. Systemic sclerosis: a prototypic multisystem fibrotic disorder. J Clin Investigation. 2007;117:557–67.
[3] Herrick AL. The pathogenesis, diagnosis and treatment of Raynaud phenomenon. Nat Rev Rheumatol. 2012;8:469–79.
[4] Abraham D, Distler O. How does endothelial cell injury start? The role of endothelin in systemic sclerosis. Arthritis Res Ther. 2007;9:S2.
[5] Hsu T, Nguyen-Tran H-H, Trojanowska M. Active roles of dysfunctional vascular endothelium in fibrosis and cancer. J Biomed Sci. 2019;26:1–12.
[6] Incalza MA, D'Oria R, Natalicchio A, Perrini S, Laviola L, Giorgino F. Oxidative stress and reactive oxygen species in endothelial dysfunction associated with cardiovascular and metabolic diseases. Vasc Pharmacol. 2018;100:1–19.
[7] Svegliati S, Spadoni T, Moroncini G, Gabrielli A. NADPH oxidase, oxidative stress and fibrosis in systemic sclerosis. Free Radic Biol Med. 2018;125:90–7.
[8] Doridot L, Jeljeli M, Chêne C, Batteux F. Implication of oxidative stress in the pathogenesis of systemic sclerosis via inflammation, autoimmunity and fibrosis. Redox Biol. 2019;25:101122.
[9] Bourji K, Meyer A, Chatelus E, Pincemail J, Pigatto E, Defraigne J-O, et al. High reactive oxygen species in fibrotic and nonfibrotic skin of patients with diffuse cutaneous systemic sclerosis. Free Radic Biol Med. 2015;87:282–9.
[10] Sambo P, Jannino L, Candela M, Salvi A, Luchetti MM, Gabrielli A, et al. Monocytes of patients with systemic sclerosis (scleroderma) spontaneously release *in vitro* increased amounts of superoxide anion. J Investig Dermatol. 1999;112:78–84.
[11] Amico D, Spadoni T, Rovinelli M, Serafini M, D'Amico G, Campelli N, et al. Intracellular free radical production by peripheral blood T lymphocytes from patients with systemic sclerosis: role of NADPH oxidase and ERK1/2. Arthritis Res Ther. 2015;17:68.
[12] Devrim E, Erten Ş, Ergüder İB, Namuslu M, Turgay M, Durak İ. Malondialdehyde and nitric oxide levels in erythrocytes from patients with systemic sclerosis. Med Princ Pract. 2008;17:349–50.
[13] Servettaz A, Guilpain P, Goulvestre C, Chereau C, Hercend C, Nicco C, et al. Radical oxygen species production induced by advanced oxidation protein products predicts clinical evolution and response to treatment in systemic sclerosis. Ann Rheumatic Dis. 2007;66:1202–9.

[14] Bochaton-Piallat M-L, Gabbiani G, Hinz B. The myofibroblast in wound healing and fibrosis: answered and unanswered questions. F1000Research. 2016;5:762.
[15] Rosenbloom J, Macarak E, Piera-Velazquez S, Jimenez SA. Human fibrotic diseases: current challenges. Methods Mol Biol. 2017;1627:1–23.
[16] Beon M, Harley R, Wessels A, Silver R, Ludwicka-Bradley A. Myofibroblast induction and microvascular alteration in scleroderma lung fibrosis. Clin Exp Rheumatol. 2004;22:733–42.
[17] Van Caam A, Vonk M, van den Hoogen F, van Lent P, van der Kraan P. Unraveling SSc pathophysiology; the myofibroblast. Front Immunol. 2018;9:2452.
[18] Manetti M, Romano E, Rosa I, Guiducci S, Bellando-Randone S, De Paulis A, et al. Endothelial-to-mesenchymal transition contributes to endothelial dysfunction and dermal fibrosis in systemic sclerosis. Ann Rheumatic Dis. 2017;76:924–34.
[19] Mendoza FA, Piera-Velazquez S, Farber JL, Feghali-Bostwick C, Jimenez SA. Endothelial cells expressing endothelial and mesenchymal cell gene products in lung tissue from patients with systemic sclerosis–associated interstitial lung disease. Arthritis Rheumatol. 2016;68:210–7.
[20] Good RB, Gilbane AJ, Trinder SL, Denton CP, Coghlan G, Abraham DJ, et al. Endothelial to mesenchymal transition contributes to endothelial dysfunction in pulmonary arterial hypertension. Am J Pathol. 2015;185:1850–8.
[21] Jimenez SA, Piera-Velazquez S. Endothelial to mesenchymal transition (EndoMT) in the pathogenesis of systemic sclerosis-associated pulmonary fibrosis and pulmonary arterial hypertension. Myth or reality? Matrix Biol. 2016;51:26–36.
[22] Thuan DTB, Zayed H, Eid AH, Abou-Saleh H, Nasrallah GK, Mangoni AA, et al. A potential link between oxidative stress and endothelial-to-mesenchymal transition in systemic sclerosis. Front Immunol. 2018;9:1985.
[23] Giordo R, Ahmed Y, Allam H, Abusnana S, Pappalardo L, Nasrallah GK, et al. EndMT regulation by small RNAs in diabetes-associated fibrotic conditions: potential link with oxidative stress. Front Cell Develop Biol. 2021;9:1275.
[24] Giordo R, Thuan DTB, Posadino AM, Cossu A, Zinellu A, Erre GL, et al. Iloprost attenuates oxidative stress-dependent activation of collagen synthesis induced by sera from scleroderma patients in human pulmonary microvascular endothelial cells. Molecules. 2021;26:4729.
[25] Giordo R, Nasrallah GK, Posadino AM, Galimi F, Capobianco G, Eid AH, et al. Resveratrol-elicited pkc inhibition counteracts nox-mediated endothelial to mesenchymal transition in human retinal endothelial cells exposed to high glucose. Antioxidants. 2021;10:224.
[26] Choi KJ, Nam J-K, Kim J-H, Choi S-H, Lee Y-J. Endothelial-to-mesenchymal transition in anticancer therapy and normal tissue damage. Exp Mol Med. 2020;52:781–92.
[27] Gorelova A, Berman M, Al Ghouleh I. Endothelial-to-mesenchymal transition in pulmonary arterial hypertension. Antioxid Redox Signal. 2021;34:891–914.
[28] Montorfano I, Becerra A, Cerro R, Echeverría C, Sáez E, Morales MG, et al. Oxidative stress mediates the conversion of endothelial cells into myofibroblasts via a TGF-β 1 and TGF-β 2-dependent pathway. Lab Invest. 2014;94:1068–82.
[29] Ma J, Sanchez-Duffhues G, Goumans M-J, Ten Dijke P. TGF-β-induced endothelial to mesenchymal transition in disease and tissue engineering. Front Cell Develop Biol. 2020;8:260.
[30] O'Brien J, Hayder H, Zayed Y, Peng C. Overview of microRNA biogenesis, mechanisms of actions, and circulation. Front Endocrinol. 2018;9:402.
[31] Catalanotto C, Cogoni C, Zardo G. MicroRNA in control of gene expression: an overview of nuclear functions. Int J Mol Sci. 2016;17:1712.
[32] Liang H, Gong F, Zhang S, Zhang CY, Zen K, Chen X. The origin, function, and diagnostic potential of extracellular microRNAs in human body fluids. Wiley Interdiscip Rev: RNA. 2014;5:285–300.
[33] Chen X, Liang H, Zhang J, Zen K, Zhang C-Y. Secreted microRNAs: a new form of intercellular communication. Trends Cell Biol. 2012;22:125–32.
[34] Hulshoff MS, del Monte-Nieto G, Kovacic J, Krenning G. Non-coding RNA in endothelial-to-mesenchymal transition. Cardiovascular Res. 2019;115:1716–31.
[35] Das A, Ganesan H, Sriramulu S, Marotta F, Kanna N, Banerjee A, et al. A review on interplay between small RNAs and oxidative stress in cancer progression. Mol Cell Biochem. 2021;476:4117–31.
[36] Li Y, Huang J, Hu C, Zhou J, Xu D, Hou Y, et al. MicroRNA-320a: an important regulator in the fibrotic process in interstitial lung disease of systemic sclerosis. Arthritis Res Ther. 2021;23:1–11.
[37] Rusek M, Michalska-Jakubus M, Kowal M, Bełtowski J, Krasowska D. A novel miRNA-4484 is up-regulated on microarray and associated with increased MMP-21 expression in serum of systemic sclerosis patients. Sci Rep. 2019;9:1–13.
[38] Henry TW, Mendoza FA, Jimenez SA. Role of microRNA in the pathogenesis of systemic sclerosis tissue fibrosis and vasculopathy. Autoimmunity Rev. 2019;18:102396.
[39] van den Hoogen F, Khanna D, Fransen J, Johnson SR, Baron M, Tyndall A, et al. Classification criteria for systemic sclerosis: an ACR-EULAR collaborative initiative. Arthritis Rheumatism. 2013;65:2737–47.
[40] Boin F, Erre GL, Posadino AM, Cossu A, Giordo R, Spinetti G, et al. Oxidative stress-dependent activation of collagen synthesis is induced in human pulmonary smooth muscle cells by sera from patients with scleroderma-associated pulmonary hypertension. Orphanet J Rare Dis. 2014;9:1–5.
[41] Fois AG, Posadino AM, Giordo R, Cossu A, Agouni A, Rizk NM, et al. Antioxidant activity mediates pirfenidone antifibrotic effects in human pulmonary vascular smooth muscle cells exposed to sera of idiopathic pulmonary fibrosis patients. Oxid Med Cell Longev. 2018;2018:2639081.
[42] Pasciu V, Posadino AM, Cossu A, Sanna B, Tadolini B, Gaspa L, et al. Akt downregulation by flavin oxidase–induced ROS generation mediates dose-dependent endothelial cell damage elicited by natural antioxidants. Toxicol Sci. 2010;114:101–12.
[43] Posadino AM, Cossu A, Giordo R, Zinellu A, Sotgia S, Vardeu A, et al. Coumaric acid induces mitochondrial damage and oxidative-mediated cell death of human endothelial cells. Cardiovascular Toxicol. 2013;13:301–6.

[44] Giordo R, Nasrallah GK, Al-Jamal O, Paliogiannis P, Pintus G. Resveratrol inhibits oxidative stress and prevents mitochondrial damage induced by zinc oxide nanoparticles in zebrafish (Danio rerio). Int J Mol Sci. 2020;21:3838.
[45] Vono R, Fuoco C, Testa S, Pirrò S, Maselli D, McCollough DF, et al. Activation of the pro-oxidant PKCβII-p66Shc signaling pathway contributes to pericyte dysfunction in skeletal muscles of patients with diabetes with critical limb ischemia. Diabetes. 2016;65:3691–704.
[46] Posadino AM, Giordo R, Cossu A, Nasrallah GK, Shaito A, Abou-Saleh H, et al. Flavin oxidase-induced ROS generation modulates PKC biphasic effect of resveratrol on endothelial cell survival. Biomolecules. 2019;9:209.
[47] Dissen GA, Lomniczi A, Neff TL, Hobbs TR, Kohama SG, Kroenke CD, et al. *In vivo* manipulation of gene expression in non-human primates using lentiviral vectors as delivery vehicles. Methods. 2009;49:70–7.
[48] Cossu A, Posadino AM, Giordo R, Emanueli C, Sanguinetti AM, Piscopo A, et al. Apricot melanoidins prevent oxidative endothelial cell death by counteracting mitochondrial oxidation and membrane depolarization. PLoS One. 2012;7:e48817.
[49] Posadino AM, Cossu A, Giordo R, Zinellu A, Sotgia S, Vardeu A, et al. Resveratrol alters human endothelial cells redox state and causes mitochondrial-dependent cell death. Food Chem Toxicol. 2015;78:10–6.
[50] Pintus G, Giordo R, Wang Y, Zhu W, Kim SH, Zhang L, et al. Reduced vasorin enhances angiotensin II signaling within the aging arterial wall. Oncotarget. 2018;9:27117–32.
[51] Xiao F, Zuo Z, Cai G, Kang S, Gao X, Li T. miRecords: an integrated resource for microRNA–target interactions. Nucleic Acids Res. 2009;37:D105–10.
[52] Kowarsch A, Preusse M, Marr C, Theis FJ. miTALOS: analyzing the tissue-specific regulation of signaling pathways by human and mouse microRNAs. Rna. 2011;17:809–19.
[53] Herrick A, Cerinic MM. The emerging problem of oxidative stress and the role of antioxidants in systemic sclerosis. Clin Exp Rheumatol. 2001;19:4–8.
[54] Abdulle AE, Diercks GF, Feelisch M, Mulder DJ, Goor Hv. The role of oxidative stress in the development of systemic sclerosis related vasculopathy. Front Physiol. 2018;9:1177.
[55] Sundaram SM, Chung L. An update on systemic sclerosis-associated pulmonary arterial hypertension: a review of the current literature. Curr Rheumatol Rep. 2018;20:1–10.
[56] Zecchin A, Kalucka J, Dubois C, Carmeliet P. How endothelial cells adapt their metabolism to form vessels in tumors. Front Immunol. 2017;8:1750.
[57] Budhiraja R, Tuder RM, Hassoun PM. Endothelial dysfunction in pulmonary hypertension. Circulation. 2004;109:159–65.
[58] Nicco C, Laurent A, Chereau C, Weill B, Batteux F. Differential modulation of normal and tumor cell proliferation by reactive oxygen species. Biomed Pharmacotherapy. 2005;59:169–74.
[59] Jimenez SA, Hitraya E, Varga J. Pathogenesis of scleroderma: collagen. Rheumatic Dis Clin North Am. 1996;22:647–74.
[60] Jinnin M. 'Narrow-sense'and 'broad-sense'vascular abnormalities of systemic sclerosis. Immunol Med. 2020;43:107–14.
[61] Medici D, Nawshad A. Type I collagen promotes epithelial–mesenchymal transition through ILK-dependent activation of NF-κB and LEF-1. Matrix Biol. 2010;29:161–5.
[62] Pinto MT, Melo FUF, Malta TM, Rodrigues ES, Plaça JR, Silva Jr WA, et al. Endothelial cells from different anatomical origin have distinct responses during SNAIL/TGF-β2-mediated endothelial-mesenchymal transition. Am J Transl Res. 2018;10:4065–81.
[63] Valenzi E, Bulik M, Tabib T, Morse C, Sembrat J, Bittar HT, et al. Single-cell analysis reveals fibroblast heterogeneity and myofibroblasts in systemic sclerosis-associated interstitial lung disease. Ann Rheumatic Dis. 2019;78:1379–87.
[64] Piera-Velazquez S, Mendoza FA, Jimenez SA. Endothelial to mesenchymal transition (EndoMT) in the pathogenesis of human fibrotic diseases. J Clin Med. 2016;5:45.
[65] Kendall RT, Feghali-Bostwick CA. Fibroblasts in fibrosis: novel roles and mediators. Front Pharmacol. 2014;5:123.
[66] Nightingale T, Cutler D. The secretion of von W illebrand factor from endothelial cells; an increasingly complicated story. J Thrombosis Haemost. 2013;11:192–201.
[67] Magenta A, Greco S, Gaetano C, Martelli F. Oxidative stress and microRNAs in vascular diseases. Int J Mol Sci. 2013;14:17319–46.
[68] Climent M, Viggiani G, Chen Y-W, Coulis G, Castaldi A. MicroRNA and ROS crosstalk in cardiac and pulmonary diseases. Int J Mol Sci. 2020;21:4370.
[69] Gong Y-Y, Luo J-Y, Wang L, Huang Y. MicroRNAs regulating reactive oxygen species in cardiovascular diseases. Antioxid Redox Signal. 2018;29:1092–107.
[70] Kim J. MicroRNAs as critical regulators of the endothelial to mesenchymal transition in vascular biology. BMB Rep. 2018;51:65–72.
[71] Long H, Wang X, Chen Y, Wang L, Zhao M, Lu Q. Dysregulation of microRNAs in autoimmune diseases: Pathogenesis, biomarkers and potential therapeutic targets. Cancer Lett. 2018;428:90–103.
[72] Shilo S, Roy S, Khanna S, Sen CK. Evidence for the involvement of miRNA in redox regulated angiogenic response of human microvascular endothelial cells. Arteriosclerosis, Thrombosis, Vasc Biol. 2008;28:471–7.
[73] Steen SO, Iversen LV, Carlsen AL, Burton M, Nielsen CT, Jacobsen S, et al. The circulating cell-free microRNA profile in systemic sclerosis is distinct from both healthy controls and systemic lupus erythematosus. J Rheumatol. 2015;42:214–21.
[74] Sing T, Jinnin M, Yamane K, Honda N, Makino K, Kajihara I, et al. microRNA-92a expression in the sera and dermal fibroblasts increases in patients with scleroderma. Rheumatology. 2012;51:1550–6.
[75] Liu RH, Ning B, Ma XE, Gong WM, Jia TH. Regulatory roles of microRNA-21 in fibrosis through interaction with diverse pathways. Mol Med Rep. 2016;13:2359–66.
[76] Zhu H, Luo H, Li Y, Zhou Y, Jiang Y, Chai J, et al. MicroRNA-21 in scleroderma fibrosis and its function in TGF-β-regulated fibrosis-related genes expression. J Clin Immunol. 2013;33:1100–9.
[77] Davis BN, Hilyard AC, Lagna G, Hata A. SMAD proteins control DROSHA-mediated microRNA maturation. Nature. 2008;454:56–61.
[78] Liu Y, Li Y, Li N, Teng W, Wang M, Zhang Y, et al. TGF-β1 promotes scar fibroblasts proliferation and transdifferentiation via up-regulating MicroRNA-21. Sci Rep. 2016;6:1–9.

[79] Zhong X, Chung AC, Chen H-Y, Meng X-M, Lan HY. Smad3-mediated upregulation of miR-21 promotes renal fibrosis. J Am Soc Nephrol. 2011;22:1668–81.
[80] Loboda A, Sobczak M, Jozkowicz A, Dulak J. TGF-β1/Smads and miR-21 in renal fibrosis and inflammation. Mediators Inflamm. 2016;2016:8319283.
[81] Leivonen S-K, Lazaridis K, Decock J, Chantry A, Edwards DR, Kähäri V-M. TGF-β-elicited induction of tissue inhibitor of metalloproteinases (TIMP)-3 expression in fibroblasts involves complex interplay between Smad3, p38α, and ERK1/2. PLoS One. 2013;8:e57474.
[82] Zanotti S, Gibertini S, Curcio M, Savadori P, Pasanisi B, Morandi L, et al. Opposing roles of miR-21 and miR-29 in the progression of fibrosis in Duchenne muscular dystrophy. Biochim Biophys Acta (BBA)-Molecular Basis Dis. 1852;2015:1451–64.
[83] Xu W, Yang Z, Lu N. A new role for the PI3K/Akt signaling pathway in the epithelial-mesenchymal transition. Cell Adhes Migr. 2015;9:317–24.
[84] Zhang Z, Zhang T, Zhou Y, Wei X, Zhu J, Zhang J, et al. Activated phosphatidylinositol 3-kinase/Akt inhibits the transition of endothelial progenitor cells to mesenchymal cells by regulating the forkhead box subgroup O-3a signaling. Cell Physiol Biochem. 2015;35:1643–53.
[85] Wei J, Feng L, Li Z, Xu G, Fan X. MicroRNA-21 activates hepatic stellate cells via PTEN/Akt signaling. Biomed Pharmacotherapy. 2013;67:387–92.
[86] Shen W, Chen G, Dong R, Zhao R, Zheng S. MicroRNA-21/PTEN/Akt axis in the fibrogenesis of biliary atresia. J Pediatric Surg. 2014;49:1738–41.
[87] Liu P, Ye Y, Wang Y, Du J, Pan Y, Fang X. MiRNA-92a promotes cell proliferation and invasion through binding to KLF4 in glioma. Eur Rev Med Pharmacol Sci. 2019;23:6612–20.
[88] Yamada NO, Heishima K, Akao Y, Senda T. Extracellular vesicles containing microRNA-92a-3p facilitate partial endothelial-mesenchymal transition and angiogenesis in endothelial cells. Int J Mol Sci. 2019;20:4406.
[89] Lu C, Shan Z, Hong J, Yang L. MicroRNA-92a promotes epithelial-mesenchymal transition through activation of PTEN/PI3K/AKT signaling pathway in non-small cell lung cancer metastasis. Int J Oncol. 2017;51:235–44.
[90] Kuroda K, Shinkai H. Gene expression of types I and III collagen, decorin, matrix metalloproteinases and tissue inhibitors of metalloproteinases in skin fibroblasts from patients with systemic sclerosis. Arch Dermatol Res. 1997;289:567–72.
[91] Wermuth PJ, Piera-Velazquez S, Jimenez SA. Exosomes isolated from serum of systemic sclerosis patients display alterations in their content of profibrotic and antifibrotic microRNA and induce a profibrotic phenotype in cultured normal dermal fibroblasts. Clin Exp Rheumatol. 2017;35:21–30.
[92] Maurer B, Stanczyk J, Jüngel A, Akhmetshina A, Trenkmann M, Brock M, et al. MicroRNA-29, a key regulator of collagen expression in systemic sclerosis. Arthritis Rheumatism. 2010;62:1733–43.
[93] Suzuki HI, Katsura A, Mihira H, Horie M, Saito A, Miyazono K. Regulation of TGF-β-mediated endothelial-mesenchymal transition by microRNA-27. J Biochem. 2017;161:417–20.
[94] Jing J, Dou T, Yang J, Chen X, Cao H, Min M, et al. Role of endothelin-1 in the skin fibrosis of systemic sclerosis. Eur Cytokine Netw. 2015;26:10–4.
[95] Xie X, Li S, Zhu Y, Liu L, Pan Y, Wang J, et al. MicroRNA-27a/b mediates endothelin-1-induced PPARγ reduction and proliferation of pulmonary artery smooth muscle cells. Cell Tissue Res. 2017;369:527–39.
[96] Kriegel AJ, Baker MA, Liu Y, Liu P, Cowley Jr AW, Liang M. Endogenous microRNAs in human microvascular endothelial cells regulate mRNAs encoded by hypertension-related genes. Hypertension. 2015;66:793–9.
[97] Callera GE, Tostes RC, Yogi A, Montezano AC, Touyz RM. Endothelin-1-induced oxidative stress in DOCA-salt hypertension involves NADPH-oxidase-independent mechanisms. Clin Sci. 2006;110:243–53.
[98] Kähler J, Mendel S, Weckmüller J, Orzechowski H-D, Mittmann C, Köster R, et al. Oxidative stress increases synthesis of big endothelin-1 by activation of the endothelin-1 promoter. J Mol Cell Cardiol. 2000;32:1429–37.
[99] Idris-Khodja N, Ouerd S, Mian MOR, Gornitsky J, Barhoumi T, Paradis P, et al. Endothelin-1 overexpression exaggerates diabetes-induced endothelial dysfunction by altering oxidative stress. Am J Hypertension. 2016;29:1245–51.
[100] Liu R-M, Desai LP. Reciprocal regulation of TGF-β and reactive oxygen species: A perverse cycle for fibrosis. Redox Biol. 2015;6:565–77.
[101] Lu Q, Wang WW, Zhang MZ, Ma ZX, Qiu XR, Shen M, et al. ROS induces epithelial-mesenchymal transition via the TGF-β1/PI3K/Akt/mTOR pathway in diabetic nephropathy. Exp Therapeutic Med. 2019;17:835–46.
[102] Son Y, Cheong Y-K, Kim N-H, Chung H-T, Kang DG, Pae H-O. Mitogen-activated protein kinases and reactive oxygen species: how can ROS activate MAPK pathways? J Signal Transduct. 2011;2011:792639.
[103] Jiao G, Pan B, Zhou Z, Zhou L, Li Z, Zhang Z. MicroRNA-21 regulates cell proliferation and apoptosis in H2O2-stimulated rat spinal cord neurons. Mol Med Rep. 2015;12:7011–6.
[104] Engedal N, Žerovnik E, Rudov A, Galli F, Olivieri F, Procopio AD, et al. From oxidative stress damage to pathways, networks, and autophagy via microRNAs. Oxid Med Cell Longev. 2018;2018:4968321.
[105] Lu B, Christensen IT, Ma LW, Wang XL, Jiang LF, Wang CX, et al. miR-24-p53 pathway evoked by oxidative stress promotes lens epithelial cell apoptosis in age-related cataracts. Mol Med Rep. 2018;17:5021–8.
[106] Manca S, Magrelli A, Cialfi S, Lefort K, Ambra R, Alimandi M, et al. Oxidative stress activation of miR-125b is part of the molecular switch for Hailey–Hailey disease manifestation. Exp Dermatol. 2011;20:932–7.